Solid-State NMR Investigation of the Structural Consequences of Plastic Deformation in Polycarbonate. 2. Local Orientational Order

Marcel Utz,[†,‡,§] Pierre Robyr,[†,‡] and Ulrich W. Suter*[,†]

Department of Materials, Institute of Polymers, and Laboratory of Physical Chemistry, ETH, CH-8092 Zürich, Switzerland

Received January 24, 2000; Revised Manuscript Received May 23, 2000

ABSTRACT: The effects of plastic deformation on conformation and local packing in polycarbonate have been quantified using polarization-transfer and double-quantum NMR methods. To within experimental precision, the conformational distribution was found to be unaffected by the deformation, whereas small changes in the local packing of molecular segments could be detected. The phenylene ring planes exhibit a tendency of orienting parallel to one another upon deformation, and the pair correlation functions between the molecular segments under study increase in amplitude at short separations. The experimental results are compared to athermal atomistic simulations, and their implications with respect to proposed heuristic models of the process of plastic deformation in polymer glasses are discussed.

1. Introduction

Despite the technological and scientific importance of the phenomenon, the plastic deformation of polymer glasses is not fully understood, and its elementary processes have not yet been identified. In the following, we report results from a solid-state NMR study of the changes in local orientational order caused by large-strain plastic deformation in glassy bisphenol-A polycarbonate.

A number of contributions reporting solid-state NMR results on polycarbonate have appeared in the literature.[1−15] Local order in the isotropic solid has been studied by one-dimensional[1] and separated local field experiements,[2−4] polarization transfer,[5] and rotational-echo double resonance.[6−9] Backbone- and ring-flip dynamics have been studied by ^{13}C line shape analysis,[10] relaxation time measurements,[11] and 2D exchange spectroscopy in the unstrained state[12] as well as under elastic tension.[13−15] The present contribution, along with a previous companion paper,[16] aims at clarifying the mechanism of plastic deformation in polycarbonate by monitoring the structural changes that it causes.

Whereas the companion paper deals with global orientational order, i.e., the orientation of molecular segments with respect to the sample frame of reference, the present contribution is concerned with *local* orientational order, specified by the relative orientation of molecular segments with respect to their neighbors.

Local orientational order in polymer glasses comes in two types. The first, also referred to as "packing", is concerned with the relative orientation of spatially proximate molecular segments. In contrast, "conformation" refers to the relative orientation of neighboring molecular segments that are covalently bound to each other. Both types of order can be quantified using suitable solid-state NMR techniques. Here, plastically deformed samples of specifically ^{13}C-enriched polycarbonate have been studied using slow MAS driven ^{13}C polarization-transfer experiments in order to measure the effect of plastic deformation on packing, and the conformational distributions before and after deformation have been determined by a double-quantum experiment. The results of this NMR study are compared to athermal atomistic simulations of the deformation process similar to the work of Mott et al.[17−19] and Hutnik et al.,[20] and the implications of the results are discussed with regards to various theoretical mechanisms of plastic deformation in glassy polymers that have been proposed in the literature.[21−24]

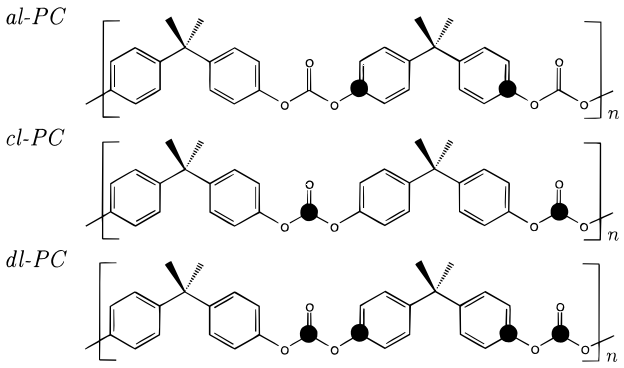

Figure 1. Repeat units of bisphenol A polycarbonate samples, enriched to 99% with ^{13}C at the positions indicated by the heavy dots. Aromatic label: al-PC; carbonate label: cl-PC; double label: dl-PC.

2. Materials and Methods

2.1. ^{13}C-Labeled Polycarbonate. The results reported in this contribution were obtained from the same samples that were studied in ref 16. The sample preparation procedure, as well as the orientation and magnitude of the relevant chemical shielding and dipolar coupling tensors, are discussed in detail in ref 16 and will only be reviewed briefly in the following. The NMR methods used here rely on polycarbonate samples specifically enriched with ^{13}C at the carbonate site (cl-PC), at the oxygen-bound phenylene site (al-PC), or both (dl-PC), as shown in Figure 1. Their synthesis has been described elsewhere.[2] Dense, rectangular specimens were produced by first precipitating the polymers from solution and, after drying, compressing the resulting powder in a rectangular mold at 250 °C for 2 min.[16] Plane-strain compression was imposed on the samples at room temperature by means of a channel die apparatus (Figure 2) fitted to a tensile testing machine. A deformation speed of $\dot{\epsilon} = -0.001\ s^{-1}$ was used in all cases.

[†] Department of Materials.
[‡] Laboratory of Physical Chemistry.
[§] Present address: Institute of Materials, Science and Department of Physics, University of Connecticut, Storrs, CT 06269.

10.1021/ma0001180 CCC: $19.00
Published on Web 08/10/2000

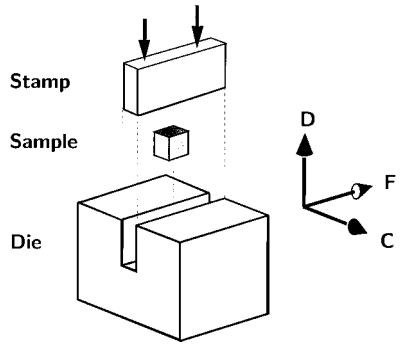

Figure 2. Schematic drawing of the channel-die-extrusion experiment. The sample (center) fits into the channel of the die. The sample is extruded in the channel by means of a stamp. The entire setup is fitted to a mechanical testing machine. The experiment produces plane strain and is characterized by the three distinct directions: F (free), C (constraint), and D (deformation).

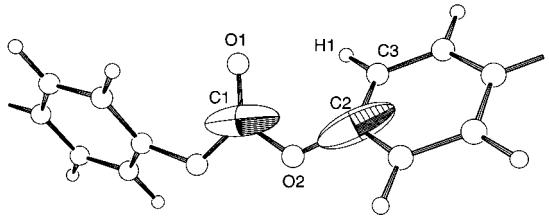

Figure 3. Ball-and-stick representation of a section of the polycarbonate chain. The ellipsoids around C1 and C2 represent the chemical shielding tensors at the carbonate and the phenylene label, respectively.

The molecular segment under study is shown in ball-and-stick representation in Figure 3. The chemical shielding tensors at the phenylene and at the carbonate site are represented as ellipsoids. At the carbonate site (C1), the *y*-axis of the chemical shielding tensor is perpendicular to the C1−O1−O2 plane, whereas the *x*-axis (most shielded) is aligned with the C1−O1 double bond (Figure 3).[2,4,25]

Apparent CSA eigenvalues at room temperature have been determined to be $\sigma_{xx} = 84.9$ ppm, $\sigma_{yy} = 120.1$ ppm, and $\sigma_{zz} = 236.4$ ppm for the carbonate site and $\sigma_{xx} = 77.9$ ppm, $\sigma_{yy} = 127.2$ ppm, and $\sigma_{zz} = 239.9$ ppm for the phenylene site.[16]

2.2. NMR Methods. ^{13}C Polarization Transfer. Packing of nearest-neighbor carbonate groups and nearest-neighbor phenylene groups before and after deformation was characterized by measuring the distance factors $f_d(\omega_1, \omega_2)$ in the two singly labeled polymers al-PC and cl-PC of Figure 1. This method has already been used to probe the packing of the undeformed samples.[5] The distance factor f_d can be defined as[26]

$$f_d(\omega_1, \omega_2) = 4\pi\rho\int_0^\infty g_{12}(r) r^{-4}\,\mathrm{d}r$$

where ρ is the density of the labeled spins and $4\pi g_{12}(r)r^2/V$ is the probability density to find a spin with resonance frequency between ω_1 and $\omega_1 + \mathrm{d}\omega_1$ and a spin with resonance frequency between ω_2 and $\omega_2 + \mathrm{d}\omega_2$ at a distance between r and $r + \mathrm{d}r$; V is the volume of the sample. According to the above definition, the contribution of a given spin pair scales as the inverse sixth power of the internuclear distance. The sensitivity of the distance factor $f_d(\omega_1,\omega_2)$ to local packing comes from the dependence of the resonance frequencies on the orientation of the molecular fragments with respect to the static magnetic field. Pairs of groups with relative orientation such that the distance between the labeled nuclei is small give large contributions to f_d at the corresponding resonance frequencies. Whereas distance factor spectra from ideally disordered samples would be flat, $f_d(\omega_1, \omega_2) =$ constant, polycrystalline solids, which are locally perfectly ordered, give rise to sharp peaks and ridge patterns.[27] For the two polymers studied here, the contributions to the distance factor come from nearest-neighbor carbons of different chain segments because of the large distance (>7 Å) between two subsequent spin-labels along the chains.[5]

The distance factors were obtained from the rate constant of polarization transfer between neighboring labeled nuclei under slow magic angle sample spinning (S-MAS) and from the intensity of the zero-quantum spectrum, both measured as a function of the two resonance frequencies.[5] The polarization-transfer rate constants were evaluated from a fit of a straight line to the off-diagonal intensities in the initial-rate regime, scaled by the respective intensities of the quasi-equilibrium spectrum. For each rate constant, eight 2D polarization-transfer experiments were used with mixing times increasing from 20 to 160 ms in 20 ms steps. Longitudinal relaxation during the mixing time was negligible. Motional contributions to the rate constants cumulatively exceeding 5% of the measured values could also be ruled out.[5] The polarization-transfer NMR measurements were carried out at 298 K on a home-built spectrometer working at a proton frequency of 300 MHz using a Chemagnetics (Fort Collins, CO) 6 mm double-resonance MAS probe. The radio-frequency fields on the ^{13}C and the H channels were both matched at 62 kHz. The MAS frequency was 50 ± 1 Hz.

Double-Quantum Spectroscopy. The DOQ-DIP method[28] employed here to measure the distribution of the dihedral angles between the two labeled sites in dl-PC (see Figure 1) is a variant of the double-quantum method introduced by Schmidt-Rohr,[29] correlating the frequencies of free double-quantum precession to single quantum coherence under a purely dipolar Hamiltonian, which is obtained by applying a multiple π-pulse sequence during signal acquisition. This has been shown to reduce the spectral width in the acquired dimension without sacrificing spectral resolution, leading to an increase in sensitivity over the original method proposed by Schmidt-Rohr.[28]

In a system of two spins $^1/_2$, double-quantum coherence evolves under the sum of the chemical shifts only and is not influenced by the dipolar coupling.[29,30] For a macroscopically isotropic dl-PC sample, the DOQ-DIP spectrum therefore depends on the distribution $P_L(\varphi_p,\varphi_c)$ of the dihedral angles $\varphi_c =$ (O1, C1, O2, C2) and $\varphi_p =$ (C1, O2, C2, C3) (cf. Figure 3). The bond lengths and bond angles in polycarbonate, which are geometrical parameters of this relationship, can be inferred from X-ray studies on low-molecular-weight analogue compounds.[31]

Deformed polymer samples are macroscopically anisotropic, and at least in principle, information on the five-dimensional distribution function $P(\phi,\theta,\chi,\varphi_p,\varphi_c)$ is contained in the DOQ-DIP spectra; ϕ, θ, χ are the Euler angles orienting the molecular frame of reference (cf. Figure 3) in the sample frame.[16] However, for the moderate degrees of plastic deformation under study here, the degree of global orientational order is quite small ($|\langle D^2_{00}\rangle| < 0.1$[16]), such that the above distribution function may be separated into a global and a local orientation part

$$P(\phi,\theta,\chi,\varphi_p,\varphi_c) \approx P_G(\phi,\theta,\chi)\, P_L(\varphi_p,\varphi_c)$$

In the present case, the global orientational order P_G was known from independent NMR measurements.[16]

The local distribution function P_L was retrieved from the DOQ-DIP NMR spectra using the conjugate-orthogonal-functions method.[28] For the deformed samples, the nonuniform global orientational distribution function P_G, known from a previous NMR study,[16] was taken into account in the calculation of the elementary DOQ-DIP spectra.

A home-built spectrometer operating at a proton resonance frequency of 220 MHz was used for the DOQ-DIP experiments. Radio-frequency field strengths of 50 and 100 kHz were used for cross-polarization and for short pulses, respectively.

2.3. Atomistic Simulation. The experimental results on conformation will be compared to an athermal atomistic model of plane strain compression in polycarbonate. In the case of packing, the distance factors of the simulations poorly repro-

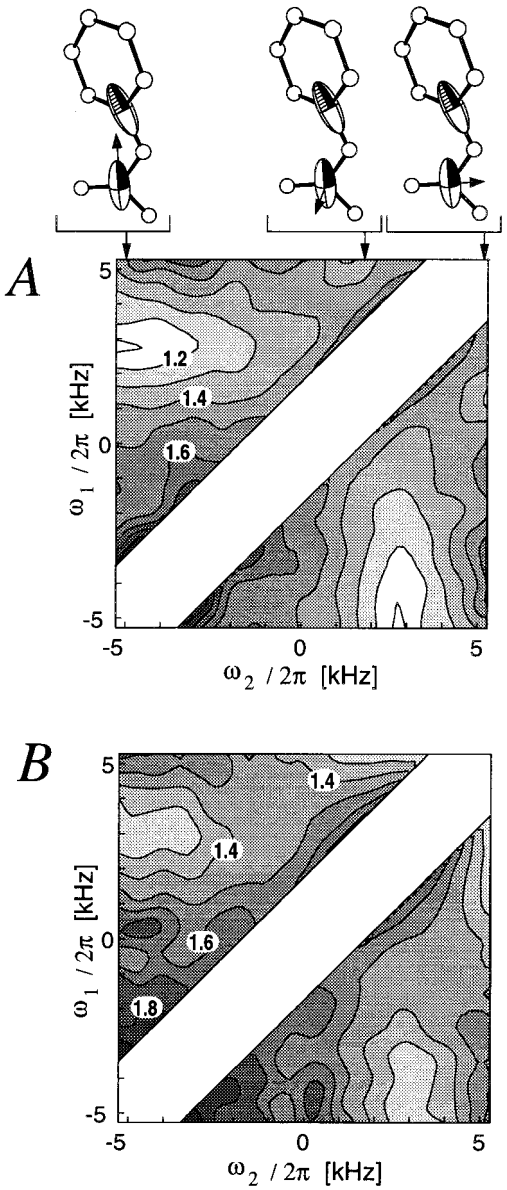

Figure 4. Distance-factor spectra of polycarbonate labeled at the carbonate site: A, before deformation; B, $\epsilon = -0.55$, constrained direction perpendicular to the magnetic field B_0. The free axis of the sample was parallel to the rotation axis.

duce those obtained experimentally already in the undeformed state,[5] so that no comparison will be made. The simulation protocol has been described in detail in ref 16. A cubic amorphous cell of polycarbonate containing seven chains of 25 repeat units each, corresponding to a cell volume of 60 nm^3, has been prepared using the packing approach of Müller and Santos et al.[32,33] This novel method is capable of efficiently generating densely packed, well-equilibrated amorphous polymer structures with dihedral angle distributions conforming to RIS probabilities. After thermalization by 50 ps of molecular dynamics at 300 K, the simulation cell was deformed in plane strain by steps of $\Delta\epsilon = -0.005$, minimizing the potential energy with respect to the internal degrees of freedom after each step.

3. Results and Discussion

3.1. Packing. The distance factors measured before and after plane-strain deformation of PC labeled at the carbonate carbons (cl-PC) are shown in Figure 4. The distance factor before deformation (Figure 4A) varies little over the spectral range. Its prominent features are the valleys along the lines with one resonance frequency close to the intermediate value of the chemical shielding tensor. The values close to the diagonal, where contributions arise from roughly parallel chain segments, and those in the region with maximal resonance-frequency difference, where intensity comes from perpendicular chain fragments, are similar. This similarity, together with the weak variation of the distance factors, shows that the local packing in PC is highly disordered with parallel and perpendicular neighboring chain segments.[5]

The distance factor of carbonate carbons after deformation resembles very much that before deformation, suggesting that little change in the local packing of the carbonate groups occurs during the deformation process. However, closer inspection reveals that the values are about 6% higher after deformation over almost the entire spectral range. This increase of the distance factor, which is also observed on average in the case of the phenylene-labeled sample, can be attributed either to an increase of the sample density or to a wider distribution of the nearest-neighbor distances after deformation. An increase in density upon plastic deformation has been observed experimentally for PC.[34] However, the changes in density reported were only about 0.3%, whereas a 10-fold larger densification would be necessary to explain the overall increase in the distance factor. It seems therefore more likely that the effect observed here is dominated by changes in the pair correlation functions between the labeled segments.

The distance factors measured in PC labeled at the phenylene groups are shown in Figure 5. The distance factor of the undeformed sample is highest in the low-frequency region, suggesting a tendency for small angles β_{zz} between C2−O2 directions of neighboring chain fragments. The local maximum of the distance factor around the high-frequency end of the diagonal may be associated with a weak preference for small angles β_{xx} between the directions perpendicular to the aromatic planes. This observation was not made in earlier measurements[5] and is most probably visible due to the higher quality of the data presented in this work. Here, polarization-transfer times up to 160 ms only have been used to calculate the initial transfer rate constants instead of 280 ms in ref 5.

The distance factors of the phenylene-labeled PC after deformation in Figure 5B,C were obtained from two different orientations of the sample in the spectrometer. For both measurements, the free direction was along the rotor axis, i.e., at 54.73° with respect to the static magnetic field, but for Figure 5B the deformation direction was in the plane defined by the rotor axis and the static field, while for Figure 5C the deformation direction was perpendicular to the static field. The two distance factors are virtually equal except for the two extremes of the antidiagonal. Although this difference indicates that some correlation exists between the local packing and the global orientation of the chain segments, it is barely significant and will not be discussed further.

In contrast to the rather uniform difference between the distance factors of the carbonate-labeled PC before and after deformation, the difference between the factors obtained from PC labeled at the phenylene groups exhibits distinct features. Close to the diagonal, the distance factors of the deformed sample are higher, especially on the high-frequency side. Approaching the

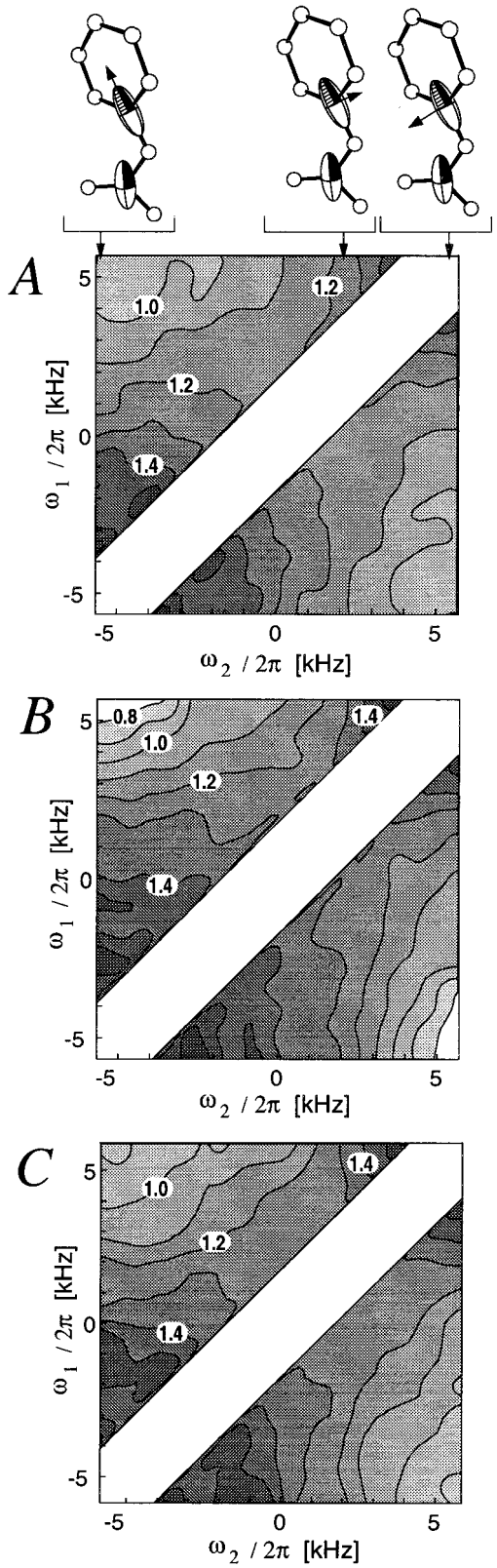

Figure 5. Distance-factor spectra of polycarbonate labeled at the phenylene site: A, before deformation; B, $\epsilon = -0.61$, constrained direction perpendicular to B_0; C, $\epsilon = -0.61$, deformation direction perpendicular to the magnetic field B_0. The free axis of the sample was parallel to the rotation axis in all three cases.

low-frequency extreme, the increase vanishes, but the plateau of high values in this region is wider after deformation. At the ends of the antidiagonal, the distance factors are lower after deformation.

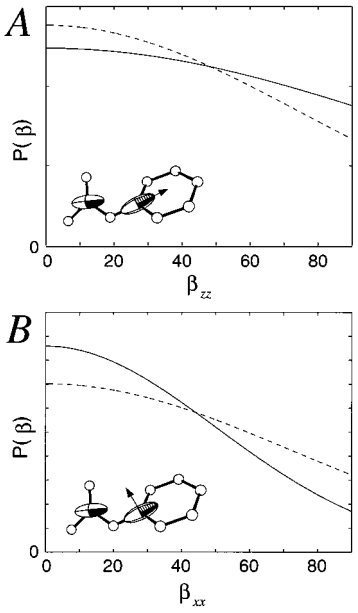

Figure 6. Distributions of angles between spatially proximate phenylene groups as determined from the distance-factor spectra in Figure 5: broken line, before deformation; solid line, $\epsilon = -0.61$; A, angle between local z directions (direction of the polymer chain); B, angle between local x directions (normal to the ring plane). Note that the distributions displayed do not contain a factor sin β, such that a completely uniform distribution would be represented by a straight line and that each contribution to the distribution is weighted by the inverse sixth power of the corresponding internuclear distance.

These observations can be explained by changes in the two-dimensional distribution of the angles β_{zz} and β_{xx}, where β_{ij} denotes the angle between the local direction i in one labeled segment and local direction j in a neighboring segment. Before discussing data fitting, it is important to note that the distance factors probe the integral of this distribution over the whole sample where each contribution is weighted with the inverse sixth power of the internuclear distance. The integrated distribution after and before deformation was obtained from a fit of a two-dimensional Gaussian line to the distance factors of Figure 5A,B. Figure 6 shows the one-dimensional projections of this two-dimensional distribution function. The half-width at half-height of the Gaussian line for β_{zz} (Figure 6A) increases from 88 ± 12° before to 128 ± **10°** after deformation; in contrast, that for β_{xx} (Figure 6B) decreases from 85 ± 12° to 59 ± 9°. The changes in local packing of the phenylene groups seem to be controlled by their oblate shape. From the ratio of the fitted factors at (5 kHz, 5 kHz), one can conclude that the mean distance between groups with parallel phenylene planes is 5% shorter after deformation. This finding is in accord with the known tendency of the phenylene ring plane normals to orient parallel to the deformation direction.[16]

3.2. Conformation. The experimental DOQ-DIP spectra of dl-PC before and after plane strain deformation of the sample are shown in Figure 7. The double-quantum spectrum appears in the ω_1 domain, whereas the ω_2 projection contains the single-quantum spectrum under a dipolar Hamiltonian. Spectral intensity vanishes at $\omega_2 = 0$ because double-quantum coherence cannot be excited in spin pairs for which the dipolar coupling is zero.

In the double-quantum domain, the spectra extend over a range of almost 20 kHz. As both CSA tensors

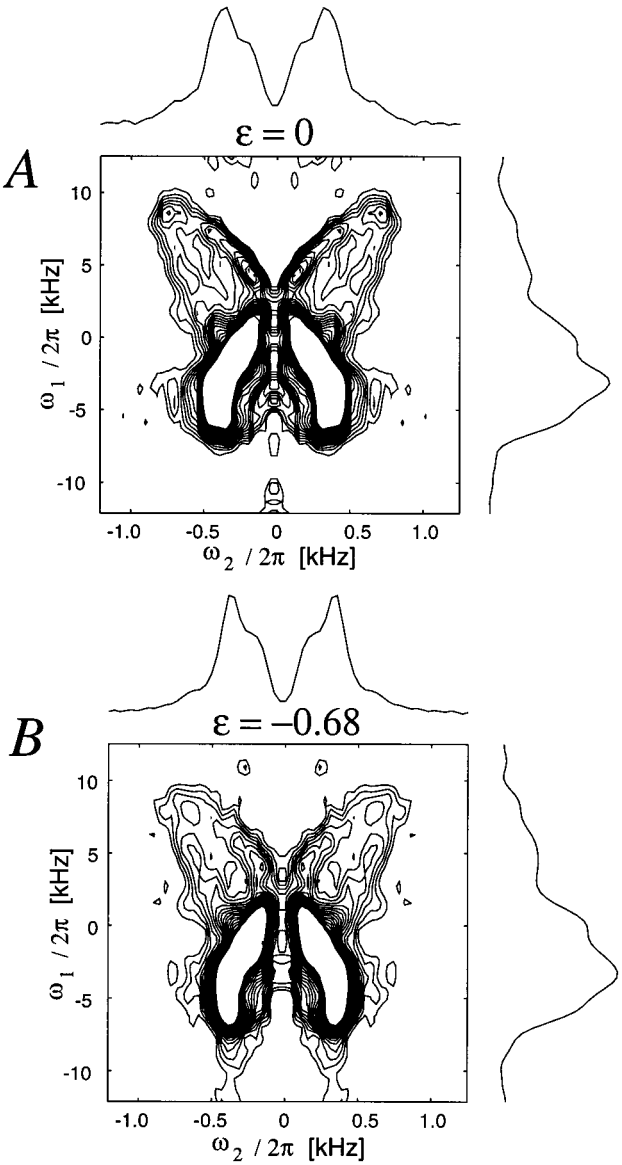

Figure 7. DOQ-DIP spectra of doubly labeled poly(carbonate) (dl-PC) recorded at 135 K before deformation (above) and after plane-strain compression to a nonrecoverable strain of $\epsilon = -0.68$. In the latter case, the spectrum has been recorded with the constrained (C) direction of the sample parallel and the free (F) direction perpendicular to the magnetic field B_0.

are about 10 kHz wide at a Larmor frequency of 55 MHz, this means that the long axes of both CSA tensors must be close to parallel for a large majority of the spin pairs in both the deformed and the undeformed samples. The conformation of the carbonate units must therefore be predominantly trans in both cases, in accord with the earlier measurements by Tomaselli et al.[2,3,35]

The close resemblance of the DOQ-DIP spectra before and after deformation (Figure 7) already shows that the conformational statistics of the carbonate unit are only slightly affected by plastic deformation. In more quantitative terms, the conformational distribution functions $P_L(\varphi_p, \varphi_c)$ obtained from the two spectra by COF analysis[28] are shown in the left column of Figure 8. In both cases, φ_c is distributed in a relatively narrow range around $\varphi_c = 0$, whereas φ_p is highly disordered. The probability density is highest at $(\varphi_p, \varphi_c) \approx (30°, 25°)$ in both cases.

Although the changes in the distribution function upon deformation are minor, some trends can be identified. The distribution of φ_c angles becomes slightly narrower, resulting in fwhm of about 90° after deformation, as opposed to about 120° before deformation (Figure 8). Also, the orientation of the phenylene planes becomes better defined upon deformation, φ_p exhibiting a pronounced peak around $\varphi_p = 0$.

To decide whether these small differences are significant, it is necessary to resort to the COF expansion coefficients p_k, $k = 1, ..., N$ (cf. Figure 9). They describe the experimental spectra as well as the corresponding distributions in terms of expansions into a sets of orthogonal basis functions, and they can be determined from the experimental spectra independently from one another by a simple projection.[28] Their error bars are estimated from the noise present in the experimental spectra. As shown in Figure 9, the error intervals of corresponding coefficients before and after deformation overlap in all cases. Therefore, within experimental precision, we must conclude that plastic deformation does not result in permanent changes in the conformational distribution function $P_L(\varphi_c, \varphi_p)$.

It is interesting to compare the experimentally determined conformational distributions to the results of atomistic simulation. The simulated dihedral angle pairs (φ_p, φ_c) are shown in Figure 10. For quantitative comparison to the experimental distributions, simulated expansion coefficients p_k^{sim} are obtained by projecting the (φ_p, φ_c) pairs onto the COF basis functions $\phi_k(\varphi_p, \varphi_c)$. Figure 9 also contains the p_k^{sim} so that the COF expansion coefficients can be compared: p_k^{NMR} to p_k^{sim}. For the simulations to be consistent with the measured data, the p_k^{sim} have to lie within the error margins of p_k^{NMR}. As shown in Figure 9, this condition is fulfilled in the undeformed case for all the coefficients shown (with the exception of p_3^{sim}, which is just below the error bar of p_3^{NMR}. After deformation, the agreement is still good for the majority of the coefficients, but a noticeable discrepancy arises in the case of p_5.

The distribution functions shown in the right column of Figure 8 have been generated from the first nine simulated expansion coefficients p_k^{sim} and can directly be compared to their experimental counterparts on the left side of Figure 8.[36] Clearly, the agreement between experiment and simulation is quite good before deformation (top row). At a deformation of $\epsilon = -0.68$, however, the simulated distribution function differs in more than details from the experimentally determined one. The simulations predict a marked sharpening of the distribution of φ_p angles, leading to a strong reduction of intensity around $(\varphi_p, \varphi_c) = (90°, 0°)$. Although a slight tendency in the same direction is visible in the experimental distribution functions, the effect is much smaller than predicted.

A similar behavior has been observed in the case of global orientational order, where athermal simulations, while qualitatively in accord with experimental results, were found to overestimate the amount of orientational order induced in the sample by plastic deformation.[16]

4. Conclusions

Using suitable solid-state NMR methods, we have quantified the local orientational order present in PC before and after large plastic deformation. The effects of deformation on both packing and conformation are small by comparison to the substantial change imposed

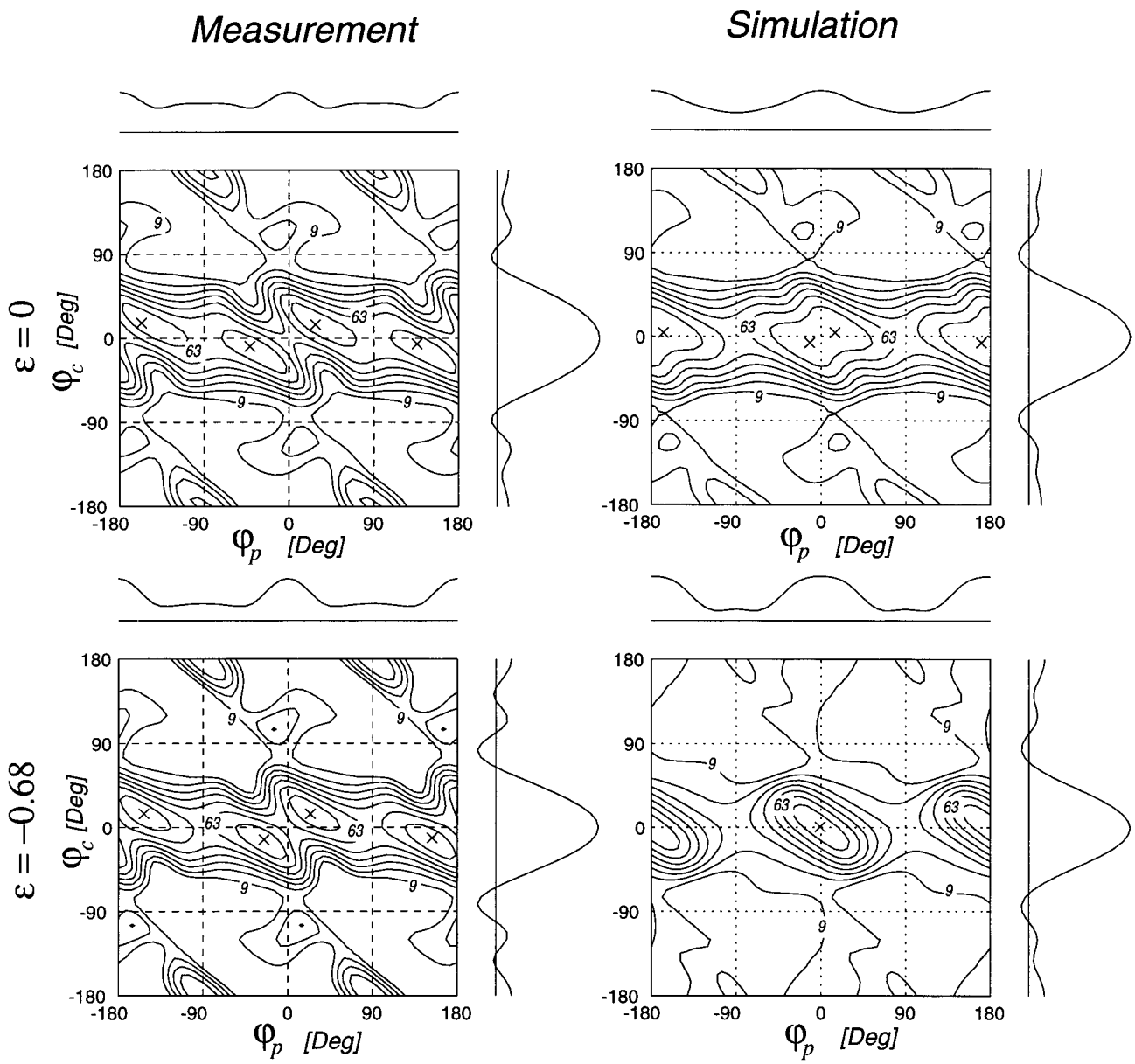

Figure 8. Left column: dihedral angle distribution functions $P_L(\varphi_c, \varphi_p)$ at $\epsilon = 0$ (top) and $\epsilon = -0.68$ (bottom) determined from the DOQ-DIP spectra in Figure 7. The first nine COF eigenfunctions have been used for the decomposition of the experimental data. Contour levels are drawn at equally spaced levels between 9% and 72% of the absolute maximum values. The locations of the maxima are shown as ×. Right column: corresponding distribution functions derived from atomistic simulation data by projection of the simulated (φ_c, φ_p) pairs onto the first nine COF eigenfunctions.

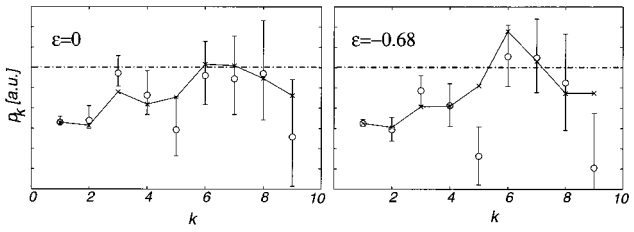

Figure 9. Conjugate-orthogonal-function (COF) expansion coefficients obtained from DOQ-DIP NMR spectra before (left) and after (right) deformation. ○ (with error bars): experimental data, coefficients obtained from DOQ-DIP NMR spectra. ×: coefficients obtained by projection of atomistic simulation data onto the COF eigenfunctions. The line linking the symbols is a guide to the eye.

on the sample shape. A tendency of the phenylene ring planes to orient parallel to each other upon deformation was detected. The two-dimensional distribution function of the dihedral angles between the carbonate and the phenylene unit in PC was found to be unaffected, to within experimental precision, by the deformation process.

Several authors have proposed models for the plastic deformation of glassy polymers.[21−23] All of those models are based on elementary processes of deformation localized to a region comparable in size to a single monomer unit. Whereas Robertson's model[21] focuses on intramolecular (conformational) aspects, the one proposed by Argon[24] takes the elastic environment of a deforming chain segment into account explicitly. In either case, the smallness of the structural changes found experimentally is difficult to reconcile with the models, as it is hard to imagine how large, localized molecular rearrangements would leave the structure of the glass unchanged on average.

The discrepancy between the smallness of changes in local order oberserved in our study and the substantial

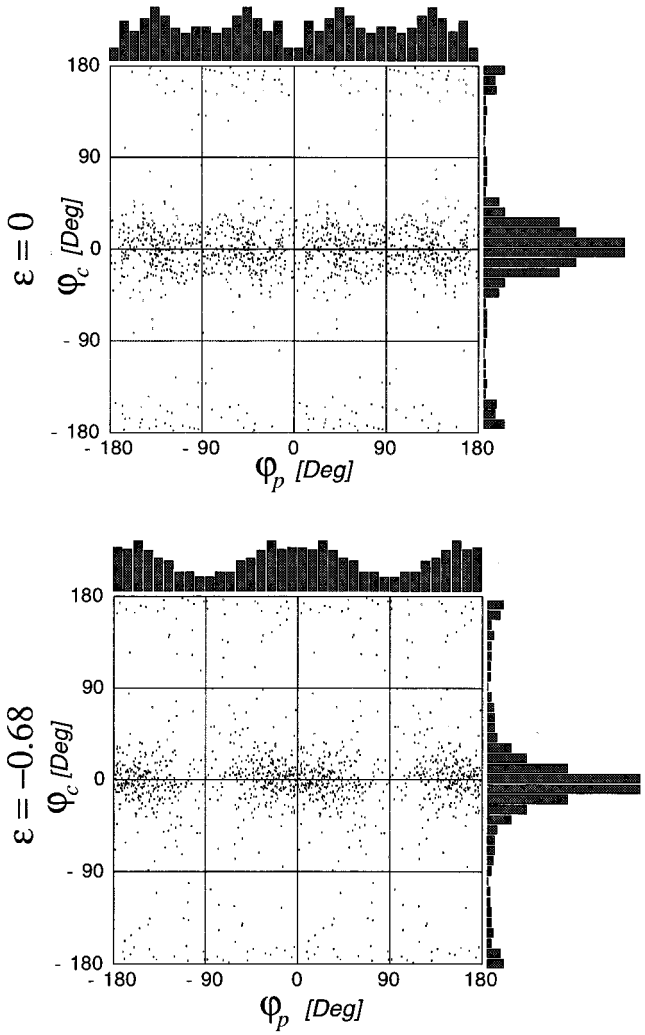

Figure 10. Scatter plots of dihedral angle pairs (φ_c, φ_p) resulting from athermal simulation: top, before deformation; bottom, $\epsilon = -0.68$.

structural modifications in the models for plastic deformation might be explained in two ways. On one hand, the elementary processes of plastic deformation in PC and other glassy polymers may be much more diffuse and cooperative than assumed in the models mentioned above. This view is supported by the results of atomistic computer simulations[18−20] which show no localization up to length scales of 40 Å. On the other hand, the local orientational order in PC might respond to plastic deformation only transiently, relaxing back to a quasi-equilibrium state on a time scale fast enough to render the changes unobservable by the experimental procedure employed here. A transient response of the conformational statistics was observed in an in-situ IR study in atactic[37] and isotactic[38] polystyrene close to the glass transition temperature. In the case under study here, the sample was deformed some 120 K below its glass transition temperature, and no appreciable strain relaxation (except for the elastic response immediately after unloading) was observed over several months. However, our results on the global orientational order that develops in PC under plastic deformation could be explained by assuming structural relaxation to be possible in PC, even at room temperature, at least up to the entanglement length scale.[16] The smallness of the observed changes in local order are entirely compatible with this assumption.

References and Notes

(1) Henrichs, P. M.; Nicely, V. A. *Macromolecules* **1990**, *23*, 3193−3194.
(2) Tomaselli, M.; Robyr, P.; Meier, B.; Grob-Pisano, C.; Ernst, R. R.; Suter, U. W. *Mol. Phys.* **1996**, *89*, 1663−1694.
(3) Tomaselli, M.; Zehnder, M. M.; Robyr, P.; Grob-Pisano, C.; Ernst, R. R.; Suter, U. W. *Macromolecules* **1997**, *30*, 3579−3583.
(4) Robyr, P.; Utz, M.; Gan, Z.; Scheurer, C.; Tomaselli, M.; Suter, U. W.; Ernst, R. R. *Macromolecules* **1998**, *31*, 5818−5822.
(5) Robyr, P.; Gan, Z.; Suter, U. W. *Macromolecules* **1998**, *31*, 6199−6205.
(6) Lee, P. L.; Schaefer, J. *Macromolecules* **1995**, *28*, 1921−1924.
(7) Lee, P. L.; Kowalewski, T.; Poliks, M. D.; Schaefer, J. *Macromolecules* **1995**, *28*, 2476−2482.
(8) Klug, C. A.; Zhu, W. L.; Tasaki, K.; Schaefer, J. *Macromolecules* **1997**, *30*, 1734−1740.
(9) Goetz, J. M.; Wu, J. H.; Yee, A. F.; Schaefer, J. *Macromolecules* **1998**, *31*, 3016−3020.
(10) Henrichs, P. M.; Linder, M.; Hewitt, M.; Massa, D.; Isaacson, H. V. *Macromolecules* **1984**, *17*, 2412−2416.
(11) Connolly, J. J.; Inglefield, P. T.; Jones, A. A. *J. Chem. Phys.* **1987**, *86*, 6602−6615.
(12) Shaefer, D.; Hansen, M.; Blimich, B.; Spiess, H. W. *J. Non-Cryst. Solids* **1991**, *130*, 777−780.
(13) Hansen, M. T.; Blümich, B.; Boeffel, C.; Spiess, H.; Morbitzer, L.; Zembrod, A. *Macromolecules* **1992**, *25*, 5542−5544.
(14) Hansen, M. T.; Spiess, H. W. *Colloid Polym. Sci.* **1993**, *271*, 446−453.
(15) Weigand, F.; Spiess, H. W. *Macromolecules* **1995**, *28*, 6361−6364.
(16) Utz, M.; Atallah, A. S.; Robyr, P.; Suter, U. W.; Ernst, R. R. *Macromolecules* **1999**, *32*, 6191−6205.
(17) Argon, A. S.; Mott, P. H.; Suter, U. W. *Phys. Status Solidi B* **1992**, *172*, 193−204.
(18) Mott, P. H.; Argon, A. S.; Suter, U. W. *Philos. Mag. A* **1993**, *67*, 931−978.
(19) Mott, P. H.; Argon, A. S.; Suter, U. W. *Philos. Mag. A* **1993**, *68*, 537−564.
(20) Hutnik, M.; Argon, A. S.; Suter, U. W. *Macromolecules* **1993**, *26*, 1097−1108.
(21) Robertson, R. E. *J. Chem. Phys.* **1966**, *44*, 3950−3956.
(22) Yannas, I. V.; Luise, R. R. In *The Strength and Stiffness of Polymers;* Zachariades, R. E., Porter, R. S., Eds.; Dekker: New York, 1983.
(23) Argon, A. S. *Philos. Mag.* **1973**, *28*, 839−865.
(24) Argon, A. S. Inelastic Deformation and Fracture of Glassy Solids. In *Materials Science and Technology;* VCH: Weinheim, 1993; Vol. 6, pp 462−508.
(25) Utz, M. Investigation of plastically deformed glassy polymers by solid-state NMR. Ph.D. Thesis, ETH Zürich, Diss No. 12717, 1998.
(26) Robyr, P.; Gan, Z.; Suter, U. W. *Macromolecules* **1998**, *31*, 8918−8923.
(27) Robyr, P.; Meier, B. H.; Fischer, P.; Ernst, R. R. *J. Am. Chem. Soc.* **1994**, *116*, 5315−5323.
(28) Utz, M. *J. Chem. Phys.* **1998**, *109*, 6110−6124.
(29) Schmidt-Rohr, K. *Macromolecules* **1996**, *29*, 3975−3981.
(30) Ernst, R. R.; Bodenhausen, G.; Wokaun, A. *Principles of Nuclear Magnetic Resonance in One and Two Dimensions;* Clarendon Press: Oxford, 1987.
(31) Perez, S.; Scaringe, R. P. *Macromolecules* **1987**, *20*, 68−77.
(32) Müller, M.; Nievergelt, J.; Santos, S.; Suter, U. W., submitted for publication.
(33) Santos, S.; Suter, U. W.; Müller, M.; Nievergelt, J., submitted for publication.
(34) Brady, T. E.; Yeh, G. S. Y. *J. Appl. Phys.* **1971**, *42*, 4622−4630.
(35) Tomaselli, M. Development and application of some NMR experiments for studying disordered solids. Ph.D. Thesis, ETH Zurich, Diss No 11455, 1996.
(36) Note also that the simulation data in Figure 10 are well represented by the truncated expansions in the right column of Figure 8, demonstrating that only nine COF eigenfunctions are sufficient to describe distribution functions at a satisfactory level of accuracy.
(37) Theodorou, M.; Jasse, B.; Monnerie, L. *J. Polym. Sci., Polym. Phys.* **1985**, *23*, 445−450.
(38) Xu, Z.; Jasse, B.; Monnerie, L. *J. Polym. Sci., Polym. Phys.* **1989**, *27*, 355−368.

MA0001180